

Numerical Study and Analytic Estimation of Forces Acting in Ballistic Gravitational Capture

Antonio Fernando Bertachini de Almeida Prado

National Space Research Institute, 12227-010 São José dos Campos, Brazil

The objective of the present paper is to study in some detail the physical reasons of the ballistic gravitational capture. A numerical study is performed to show the magnitude of the forces involved in the ballistic gravitational capture as a function of time. It shows that the resultant force is near zero all of the time. Then, this phenomenon is explained in terms of the integration of the perturbing forces with respect to time. The relation between those integrals and the reduction of the two-body energy with respect to the moon is derived and applied to a large set of trajectories. Analytical equations for those forces are derived to estimate their magnitude and to show the best directions of approach for the ballistic gravitational capture. Using those equations, an analytical estimate of the effects for different values of the mass parameter of the couple of primaries is derived.

Introduction

THE ballistic gravitational capture is a characteristic of some dynamical systems in celestial mechanics as in the restricted three-body problem that is considered in this paper. The basic idea is that a spacecraft (or any particle with negligible mass) can change from a hyperbolic orbit with a small positive energy around a celestial body into an elliptic orbit with a small negative energy without the use of any propulsive system. The force responsible for this modification in the orbit of the spacecraft is the gravitational force of the third body involved in the dynamics. In this way this force is used as a zero cost control, equivalent to a continuous thrust applied in the spacecraft. One of the most important applications of this property is the construction of trajectories to the moon.

The application of this phenomenon in spacecraft trajectories is recent in the literature. The first demonstration of this was in 1987 (Belbruno¹). Further studies include Belbruno,^{2,3} Krish,⁴ Krish et al.,⁵ Miller and Belbruno,⁶ and Belbruno and Miller.^{7,8} They all studied missions in the Earth–moon system that use this technique to save fuel during the insertion of the spacecraft in its final orbit around the moon. Another set of papers that made fundamental contributions in this field, also with the main objective of constructing real trajectories in the Earth–moon system, are those of Yamakawa and coworkers^{9–11} and Kawaguchi.¹² The first real application of a ballistic capture transfer was made during an emergency in a Japanese spacecraft.¹³ After that, some studies that consider the time required for this transfer appeared in the literature. Examples of this approach can be found in the papers by Vieira Neto and Prado.^{14,15} An extension of the dynamical model to consider the effects of the eccentricity of the primaries is also available in the literature.^{16,17} A study of this problem, from the perspective of invariant manifolds, was developed by Belbruno¹⁸ in 1994. An application for a mission

to Europa is shown in Ref. 19. Very recent studies on this topic are available in Refs. 20–24. In particular, they include a numerical proof of the existence of the invariant manifold structure²⁰ and an analytic estimation of the weak stability boundaries.^{21,22}

Examining the literature related to the weak stability boundaries, one finds several definitions of ballistic gravitational capture, depending on the dynamical system considered. Those differences exist to account for the different behavior of the systems. In the restricted three-body problem the system considered in the present paper, ballistic gravitational capture is assumed to occur when the massless particle stays close to one of the two primaries of the system for some time. A permanent capture is not required because in this model it does not exist, and the phenomenon is always temporary, which means that after some time of the approximation the massless particle escapes from the neighborhood of the primary.

For the practical purposes of studying spacecraft trajectories, the majority of the papers available in the literature study this problem looking at the behavior of the two-body energy of the spacecraft with respect to the moon. A quantity called C_3 (that is twice the total energy of a two-body system) is defined, with respect to the closer primary, by

$$C_3 = V^2 - 2\mu/r \quad (1)$$

where V is the velocity of the spacecraft relative to the closest primary, r is the distance of the spacecraft from this primary, and μ is the dimensionless gravitational parameter of the primary considered. From the value of C_3 , it is possible to know if the orbit is elliptical ($C_3 < 0$), parabolic ($C_3 = 0$), or hyperbolic ($C_3 > 0$) with respect to the moon. Based upon this definition, it is possible to see that the value of C_3 is related to the velocity variation ΔV needed to insert the spacecraft in its final orbit around the moon. In the case of a spacecraft approaching the moon, it is possible to use the



Dr. Antonio F. B. A. Prado is the Academic Coordinator and Professor of the Aerospace Engineering Graduate School at the National Institute for Space Research (INPE) in Brazil. He was born in Jau (Brazil). He received the following academic degrees: Ph.D. (1993) and M.S. (1991) in Aerospace Engineering from the University of Texas at Austin (USA), M.S. in Space Science (1989) from INPE (Brazil), B.S. in Physics (1986) and Chemical Engineer (1985) from the University of São Paulo (Brazil). He is member of the Tau-Beta-Pi National Engineering Honor Society and of the Honor Society of Phi-Kappa-Phi. He received the Wagner Sessin prize in the field of Orbital Mechanics and Control for Brazilian young researchers in November, 2000; PRADO@DEM.INPE.BR.

gravitational force of the Earth to lower the value of C_3 with respect to the moon, and so the fuel consumption required to complete this maneuver is reduced. In that way the search for trajectories that arrive at the moon with the maximum possible value for the reduction of C_3 is very important. In the majority of the studies relative to this problem, a numerical approach of verifying the values of C_3 during the trajectory is used to identify useful trajectories. Because the trajectories are very sensitive to the initial conditions, it is convenient to start the propagation of the trajectories at the point of closest approach to the moon and propagate the trajectories with a negative time step. If there is a change of sign in C_3 from negative (closed trajectory) to positive (open trajectory), this trajectory is considered an escape in the backward sense of time. It means that a ballistic gravitational capture occurs in the positive sense of time, and this particular trajectory can be used to reduce the amount of fuel in an Earth-moon transfer. Although frequently used in the literature, the backward integration is not the only possible way to study this problem, and a forward algorithm can be found in Ref. 25.

The present paper has two main goals: 1) to explain this phenomenon based on the integration of the perturbative forces with respect to time and 2) based upon that explanation to develop analytical equations to estimate the numerical results, which allows the derivation of an equation that estimates the reduction of C_3 as a function of the masses of the primaries.

Mathematical Model

For the numerical simulations shown in this paper, the model used is the planar restricted three-body problem. The system considered for all of the simulations shown in this paper is the Earth-moon system because this is the system with more likely applications of the ballistic gravitational capture technique. The standard canonical system of units is used, in which the unit of distance is the distance between M_1 (the Earth) and M_2 (moon); the angular velocity ω of the motion of M_1 and M_2 is set to unity; the mass of the smaller primary M_2 is given by $\mu = m_2/(m_1 + m_2)$ (where m_1 and m_2 are the real masses of M_1 and M_2 , respectively) and the mass of M_2 is $(1 - \mu)$; the unit of time is defined such that the period of the motion of the two primaries is 2π and the gravitational constant is unity.

There are several customary systems of reference for studying this problem.²⁶ In this paper the rotating system is used because it is the one that has well-known equations of motion and a simple expression for the Jacobian constant, which allows the verification of the accuracy of the numerical integration. This system has the following characteristics: origin at the center of mass of the two primaries; horizontal axis lying in the line connecting the two primaries, pointing to M_2 ; vertical axis perpendicular to the plane of motion of the two primaries. Based upon those conventions, the equations of motion for the spacecraft are²⁶

$$\ddot{x} - 2\dot{y} = \frac{\partial \Omega}{\partial x} \quad (2)$$

$$\ddot{y} + 2\dot{x} = \frac{\partial \Omega}{\partial y} \quad (3)$$

where Ω is the pseudo-potential given by

$$\Omega = \frac{1}{2}(x^2 + y^2) + (1 - \mu)/r_1 + \mu/r_2 \quad (4)$$

The symbols r_1 and r_2 are the distances between the spacecraft and the Earth and the moon, respectively. There are several definitions of the Jacobian constant.²⁶ In this paper the definition used is (where V is the velocity of the spacecraft)²⁶

$$J = 2(1 - \mu)/r_1 + 2\mu/r_2 + (1 - \mu)r_1^2 + \mu r_2^2 - V^2 \quad (5)$$

To avoid numerical problems during the close encounters with the primaries, the Lemaître regularization²⁶ is used in the equations of motion of the spacecraft. A more detailed description to obtain the equations of motion for this situation is available in Ref. 27, where several trajectories obtained under this model are also shown.

The usual approach to study those trajectories is to start the numerical integration at the point of closest approach to the moon. At this point a certain negative value of C_3 is assigned to the spacecraft, and its velocity vector is computed from Eq. (1), assuming that the

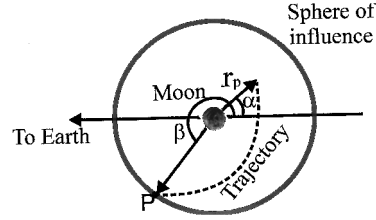


Fig. 1 Parameters of the ballistic gravitational capture.

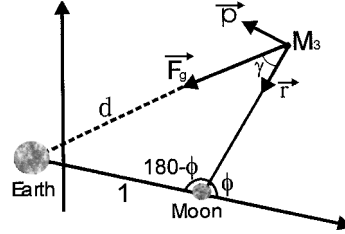


Fig. 2 Gravitational force of the Earth.

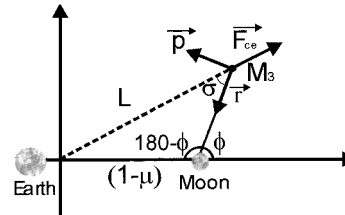


Fig. 3 Centrifugal force.

distance r is known and that the velocity vector has null radial velocity. In this way the spacecraft starts its motion close to the moon, and a negative time step in the numerical propagation of the trajectory is used to determine its motion before the closest approach. The final conditions of the trajectory were converted into the initial conditions to study the problem. Then, during the numerical integration process a trajectory is considered a ballistic gravitational capture when the distance from the moon reaches 100,000 km in a time less than 50 days.¹¹ This distance will define the gravitational sphere of capture of the moon. The main parameters of the trajectory are shown in Fig. 1. In this figure r_p is the periapsis distance (assumed to be 1838 km in the calculations performed in the present paper), α is the periapsis position angle that specifies the point of closest approach with the Moon, and β is the entry position angle that specifies the point where the spacecraft reaches the sphere of capture of the moon. In this figure it is shown as a direct capture (counterclockwise), but it is also possible to have a retrograde capture (clockwise).

Forces Involved in the Dynamics

To understand better the physical reasons of this phenomenon, it is useful to calculate the forces acting over the massless particle. Figure 2 shows the gravitational force F_g of the Earth acting in a spacecraft M_3 that is approaching the moon, and Fig. 3 shows the centrifugal force acting in the same situation. There is also the coriolis force, given by $-2\omega \times V$, where ω is the angular velocity of the reference system and V is the velocity of the spacecraft. This force is included in the numerical simulations, but it is not analyzed in detail because the main idea of this paper is to explain the ballistic gravitational capture as a result of perturbative forces acting in the direction of motion of the spacecraft and the coriolis force acts perpendicular to the direction of motion of the spacecraft all of the time. In this way it does not contribute to the phenomenon studied here. Later in this paper this force is considered, to analyze accelerations perpendicular to the radial direction. The direction r points directly to the center of the moon, and the direction p is perpendicular to r , pointing in the counterclockwise direction. The distance between the spacecraft and the Earth is d , the angle formed by the line connecting the Earth to the spacecraft and the direction r is γ . The angle ϕ is used to define instantaneously the direction r . From geometrical considerations in Figs. 2 and 3, it is possible to write

$$|F_g| = (1 - \mu)/d^2 \Rightarrow F_g = [(1 - \mu)/d^2] \cos \gamma r + [(1 - \mu)/d^2] \sin \gamma p \quad (6)$$

Applying the law of cosines,

$$1 = d^2 + r^2 - 2dr \cos \gamma \Rightarrow \cos \gamma = \frac{1 - d^2 - r^2}{-2rd} \quad (7)$$

But

$$d^2 = 1 + r^2 - 2r \cos(180^\circ - \phi) = 1 + r^2 + 2r \cos \phi \quad (8)$$

From Eqs. (7) and (8)

$$\begin{aligned} \cos \gamma &= \frac{1 - 1 - r^2 - 2r \cos \phi - r^2}{-2rd} \\ &= \frac{2r^2 + 2r \cos \phi}{+2rd} = \frac{r + \cos \phi}{d} \end{aligned} \quad (9)$$

From the law of sines,

$$\frac{d}{\sin(180^\circ - \phi)} = \frac{1}{\sin \gamma} \Rightarrow \sin \gamma = \frac{\sin \phi}{d} \quad (10)$$

Then, using Eqs. (9) and (10),

$$\begin{aligned} \mathbf{F}_g &= \frac{(1 - \mu)(r + \cos \phi)}{d^3} \mathbf{r} + \frac{(1 - \mu) \sin \phi}{d} \mathbf{p} \\ &= \frac{(1 - \mu)(r + \cos \phi)}{(1 + r^2 + 2r \cos \phi)^{\frac{3}{2}}} \mathbf{r} + \frac{(1 - \mu) \sin \phi}{(1 + r^2 + 2r \cos \phi)^{\frac{1}{2}}} \mathbf{p} \end{aligned} \quad (11)$$

For the centrifugal force the expression is

$$\mathbf{F}_{ce} = -F \cos \sigma \mathbf{r} + (-F \sin \sigma) \mathbf{p} \quad (12)$$

where $F = \omega^2 L = L$ (because $\omega = 1$).

By analogy with the gravitational force,

$$\cos \sigma = \frac{(1 - \mu)^2 - L^2 - r^2}{-2rL} \quad (13)$$

But, it is also known that $L^2 = (1 - \mu)^2 + r^2 + 2r(1 - \mu) \cos \phi$; therefore,

$$\begin{aligned} \cos \sigma &= \frac{(1 - \mu)^2 - (1 - \mu)^2 - r^2 - 2r(1 - \mu) \cos \phi - r^2}{-2rL} \\ &= \frac{r + (1 - \mu) \cos \phi}{L} \end{aligned} \quad (14)$$

From the law of sines,

$$\frac{L}{\sin(180^\circ - \phi)} = \frac{(1 - \mu)}{\sin \sigma} \Rightarrow \sin \sigma = \frac{\sin \phi (1 - \mu)}{L} \quad (15)$$

Combining all of the results together,

$$\mathbf{F}_{ce} = -[r + (1 - \mu) \cos \phi] \mathbf{r} + (\mu - 1) \sin \phi \mathbf{p} \quad (16)$$

Physical Explanation of the Ballistic Gravitational Capture

During the approach phase, when the spacecraft is close to the moon, the force that dominates the dynamics is caused by the central body (the moon). All others forces are perturbations on the motion of the massless particle. In the model considered here the perturbations are caused by the gravitational force of the Earth and the centrifugal force caused by the rotation of the system. The coriolis force also acts in the massless particle, but it does not have any component in the direction of motion, as explained before. In that way a method to understand the behavior of the perturbing forces is to study the components of each force during the approach phase. The forces involved are divided in the radial and transverse components. After that they are projected in the direction of motion of the massless particle because this is the component that explains the ballistic gravitational capture phenomenon. The conventions used in this paper imply that in the radial direction the positive sign means the force is acting in the direction of the moon and that in the transverse direction the positive sign indicates the force is acting in the

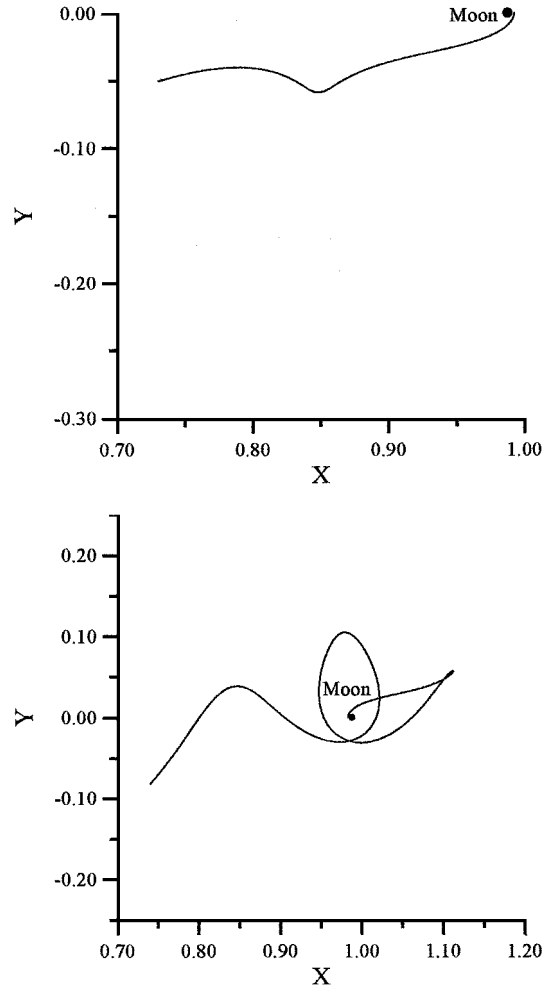


Fig. 4 Trajectories with $C_3 = -0.2$ ($\alpha = 0$ deg above and $\alpha = 180$ deg below) in canonical units.

counterclockwise direction. When the direction of motion is considered, the force is positive when applied in the direction of the motion of the particle and negative if applied against the direction of motion. The trajectories are studied only from the periapsis at the moon until the sphere of capture. This is because the main interest here is the trajectories that use a swing-by with the moon to reduce the total fuel consumption of the mission. In this type of maneuver, after the spacecraft reaches the sphere of capture of the moon an impulsive maneuver is applied to send the spacecraft to a swing-by with the moon. Those two events change the behavior of the system. Therefore, this technique allows us to separate the complete transfer into three distinct phases, one of them the ballistic gravitational capture that is studied here.

To exemplify the problem studied, two trajectories ending in ballistic gravitational captures are computed and plotted in Fig. 4. For these two trajectories the procedure of backward integration starting with the velocity perpendicular to the position vector was used. So, from the value of C_3 that is assumed (-0.2 in both trajectories) and the periapsis distance chosen for the trajectories (1838 km for both trajectories, which means 100 km from the surface of the moon), Eq. (1) is used to compute the magnitude of the velocity vector. This value, together with the assumption that the velocity is perpendicular to the periapsis distance, allows the calculation of the velocity vector. The values for the angle α used are 0 deg for the first trajectory and 180 deg for the second trajectory. Those values are used because they are among the angles that give the maximum value for the savings obtained in this maneuver.¹¹ As explained before, the time step used for the numerical integration is negative so that the instant when the time is zero represents the moment that the particle is at the periapsis. The plots shown to represent the trajectories are in dimensionless canonical units. The value of the Jacobian

constant for both trajectories, calculated by Eq. (5), is 3.1847. The value for the Jacobian constant for the Lagrangian point that exist between the Earth and the moon is²⁶ 3.2003, and so the condition that the value for the trajectory must be lower than the value at this Lagrangian point is satisfied. The value for the Lagrangian point that exists behind the moon is 3.1841, which means that the trajectories shown have a Jacobian constant a little bit above it. This is consistent with the fact that both trajectories approach the moon from the side of the Earth. If the value for the initial C_3 is -0.1954 ($-0.2 \text{ km}^2/\text{s}^2$), as used in Ref. 11, the Jacobian constant is 3.1801, which is below the value 3.1841 and the spacecraft can approach the moon from all directions.

Figure 5 shows the behavior of the forces acting on the spacecraft for those trajectories. The curves are 1) gravitational radial force, 2) gravitational transverse force, 3) centrifugal radial force, 4) centrifugal transverse force, 5) resultant radial force, 6) resultant transverse force, 7) gravitational force in the direction of motion, 8) centrifugal force in the direction of motion, 9) resultant force in the direction of motion. For the first trajectory the radial direction of the force caused by the gravitational attraction of the Earth has a negative sign, thus reducing the velocity of the spacecraft during the approach. In the transverse direction this force is also negative, which means that it is acting to accelerate the spacecraft in the clockwise direction. In the direction of motion, the sign is also negative, which means that it is braking the spacecraft during the whole trajectory. The centrifugal force acts in an opposite direction from the gravity force caused by the Earth, but with smaller absolute values. It means that the gravity force of the Earth, which causes the

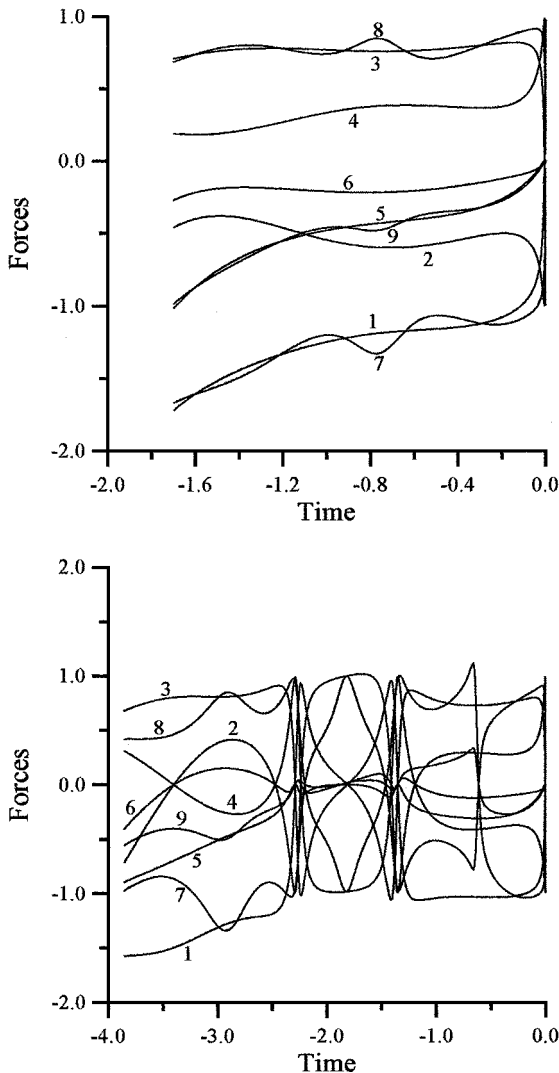


Fig. 5 Forces (canonical units) involved in the trajectories with $C_3 = -0.2$ ($\alpha = 0$ deg above and $\alpha = 180$ deg below).

spacecraft to reduce its velocity, dominates the perturbation on the motion of the spacecraft. The resultant on the transverse direction accelerates the spacecraft in the clockwise direction. The analyses of the second trajectory are more complicated because this trajectory makes several loops before reaching the moon and it causes alteration of the signs of the forces during the trajectory. So, during most of the time the value of C_3 decreases, but in some parts of the trajectory it increases. Those parts correspond to the instants where the curve 9 (resultant of the forces in the direction of the motion) is positive. The final result is a decrease in the value of C_3 . Figure 6 shows the value of C_3 as a function of the distance between the spacecraft and the moon. It shows that the decrease of C_3 occurs during the whole trajectory and the loops around the moon occur when C_3 was already reduced to a negative value close to -0.2 , the final value. Figure 7 shows the integral with respect to the time of the forces acting in the directions of motion of the spacecraft in trajectories with initial value of $C_3 = -0.15$. For those trajectories the value of the Jacobian constant is 3.1348. The three lines in the figure show the gravitational force caused by the Earth, the centrifugal and the resultant force. The regions where there are no points correspond to trajectories that collide with the moon before escape, and they do not exist in reality. To make this figure, 180 trajectories were simulated with a step of 2 deg between two consecutive values of α in the initial conditions. This figure shows some interesting characteristics of this phenomenon: 1) the integral of the resultant

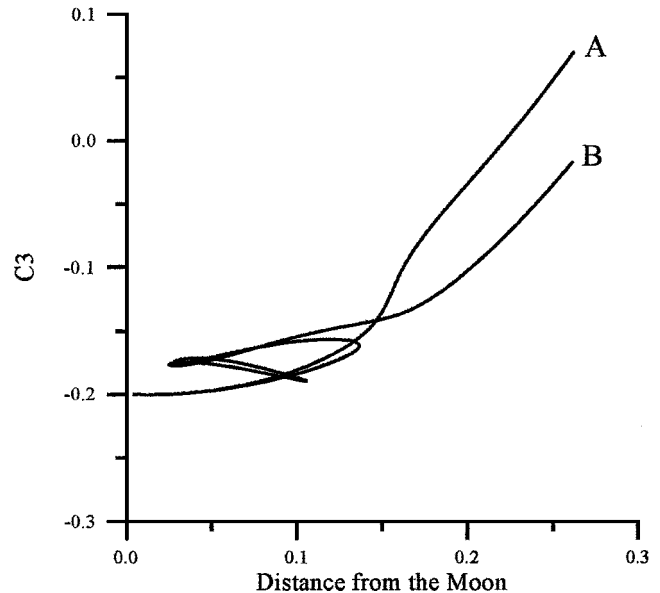


Fig. 6 Value of C_3 as a function of the distance from the moon (A: $\alpha = 0$ deg, B: $\alpha = 180$ deg).

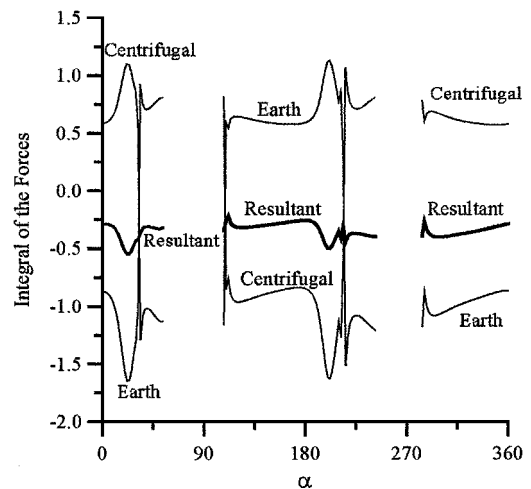


Fig. 7 Integral of the forces studied in the direction of motion of the spacecraft as a function of α .

force is always negative, which means that the spacecraft is always decelerated after one complete trajectory; 2) the two perturbative forces always have effects opposite to each other; 3) there are a few points of maximum effect, where the reduction of C_3 is larger.

The relation between the forces and the variation of C_3 can be explained in terms of fundamental physical laws. Suppose that the value of C_3 at the periapsis is called C_{3p} , and its value at the crossing point with the sphere of capture of the Moon is called C_{3sc} . From the definition of C_3 [Eq. (1)], the results are

$$C_{3p} = V_p^2 - 2\mu/r_p \quad (17)$$

$$C_{3sc} = V_{sc}^2 - 2\mu/r_{sc} \quad (18)$$

where the subscript sc stands for values at the sphere of capture of the moon.

The effects of the three forces studied in the system (gravitational—Earth and moon—and centrifugal) is to change the velocity of the spacecraft according to the physical law

$$\int_{t_0}^{t_f} F dt = (V_f - V_0) \quad (19)$$

where F is the force per unit mass of the spacecraft, V_0 is the velocity at t_0 , and V_f is the velocity at t_f . Then, defining the variation of C_3 (ΔC_3) between the periapsis and the sphere of capture of the moon as $C_{3p} - C_{3sc}$ and applying Eq. (19) between the same instants to write V_{sc} in terms of V_p we have

$$\begin{aligned} \Delta C_3 = C_{3p} - C_{3sc} &= V_p^2 - 2\mu/r_p - (V_p - I_{tot})^2 + 2\mu/r_{sc} \\ &= 2\mu(1/r_{sc} - 1/r_p) + 2V_p I_{tot} - I_{tot}^2 \end{aligned} \quad (20)$$

where I_{tot} represents the time integral of the resultant effects of the three forces studied in this system in the direction of the motion of the spacecraft. Equation (20) gives the variation of C_3 in the rotating frame because I_{tot} is evaluated in this system. The final desired result is the variation of C_3 in the inertial system. To obtain this quantity, it is necessary to follow the steps: 1) give an initial value of C_3 in the inertial frame to start the computation of the trajectory; 2) convert this value to its correspondent value in the rotating frame, using the equation

$$\begin{aligned} C_{3inertial} &= C_{3rotating} + 2(x\dot{y} - \dot{x}y) + x^2 \\ &\quad + y^2 - 2(1 - \mu)(x + \dot{y}) + (1 - \mu)^2 \end{aligned} \quad (21)$$

3) propagate the trajectory, computing the forces at every instant of time and integrating their effects in time. This integration is performed by dividing the trajectory into small steps of time and adding the product of the force and the time step. The step used in the simulations shown here is 0.0001 in regularized units of time; 4) use Eq. (20) to obtain the final value of C_3 in the rotating frame; 5) use Eq. (21) to convert this value to its equivalent in the inertial frame, and so obtaining the desired variation of C_3 in this reference frame.

For the two trajectories shown in Fig. 4, the computed values for the variation of C_3 and the values obtained by the algorithm just described are, respectively, -0.2656 and -0.2658 for the first trajectory and -0.1802 and -0.1806 for the second trajectory. Numerical simulations using smaller steps of time were performed, and the results showed that the difference between those values goes to zero with the reduction of the step size. Figure 8 shows the variation of C_3 for a series of 180 trajectories, with the initial values of α spaced 2 deg apart. The values computed by the algorithm and the values measured are plotted in Fig. 8, but they are so close to each other that they are not visible as two individual lines. Those experiments validate the proposed mechanism to explain the ballistic gravitational capture as a result of the action of an acceleration field that acts analogously to a low thrust engine decelerating the spacecraft over the time.

Analytical Analyses of the Forces

The next step of this research is to develop analytical expressions for the components of each force, in order to obtain an estimate of

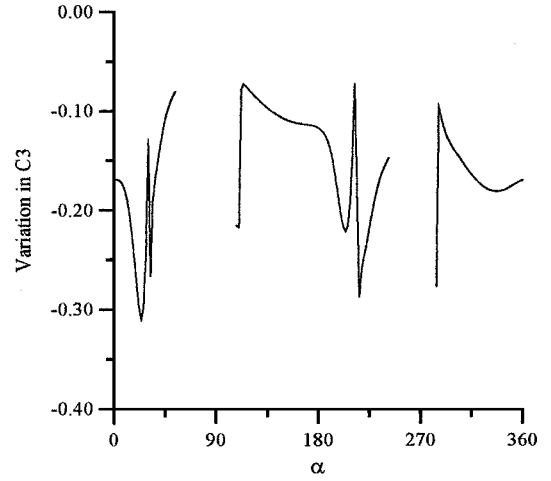


Fig. 8 Variation of C_3 of the spacecraft as a function of α .

their effects. The main idea is to estimate the potential of the field around the moon to reduce the value of C_3 and not to make predictions for a single trajectory. The analytical equations to measure the effects of this perturbation are derived under the assumption that the trajectory followed by the spacecraft is an idealized trajectory that does not deviate from the radial direction. The real trajectories are not radial, as can be seen in Fig. 4 and in equivalent results shown in the literature, but the equations derived under this assumption can be used to: 1) estimate the values of the possible reductions in the value of C_3 , not only for the Earth–moon system, but for any system of primaries, as shown later in this paper; 2) show the existence of directions of motion that results in larger reductions of C_3 , thereby mapping analytically the decelerating field that exists in the neighborhood of the moon; and 3) estimate the effects of the periapsis distance and the size of the sphere of capture because the equations derived are explicitly functions of those parameters. Another justification for the radial trajectories used to derive the equations is that the reduction of C_3 is a result of the effects of the forces in time during the whole trajectory, and even for trajectories that show several loops before arriving at the periapsis (Fig. 4) during most of the time the trajectory can be seen as composed of a set of trajectories close to radial. Figure 6 shows that when the spacecraft starts to perform loops around the moon C_3 has already achieved approximately 85% of its total reduction.

For the derivation performed here, the same components measured by the numerical analysis are calculated: the radial (the direction of motion under the assumption used here) and transverse directions. Then, assuming that the spacecraft is in freefall (subject only to the gravitational and centrifugal forces) traveling with zero energy (parabolic trajectory) and that the trajectories do not deviate from a straight line the result is

$$\text{total energy} = E = 0 = \frac{1}{2}V^2 - \frac{\mu}{r} \Rightarrow V = \sqrt{\frac{2\mu}{r}} = \frac{ds}{dt} \quad (22)$$

Here ds is the distance traveled by the particle during the time dt . To obtain the integral of the effect of the perturbing forces with respect to time, it is possible to perform the calculations in terms of the radial distance by making the substitution

$$\int_{t_0}^{t_f} F dt = \int_{S_0}^{S_f} \left(\frac{F}{V} \right) ds = \int_{r_{\min}}^{r_{\max}} \left(\frac{F}{V} \right) dr \quad (23)$$

The extreme points of the integration change position (S_0 becomes $r_{\min} = r_p$ = periapsis distance and S_f becomes $r_{\max} = r_{sc}$ = distance for the sphere of capture) here and in all of the following integrations to take into account that the positive sense of the radial direction points toward the moon. Because the spacecraft is assumed to approach the moon on a radial trajectory, the result $\phi = \alpha = \beta$ is valid, and the variable α is used as the independent parameter. Then, for the radial component of the Earth's gravity

$$F_g = \frac{(1 - \mu)(r + \cos \alpha)}{(1 + r^2 + 2r \cos \alpha)^{\frac{3}{2}}}$$

the integral is

$$F_1(\alpha) = \int_{r_{\min}}^{r_{\max}} \frac{(1 - \mu)(r + \cos \alpha)}{(1 + r^2 + 2r \cos \alpha)^{\frac{3}{2}} (2\mu/r)^{\frac{1}{2}}} dr \quad (24)$$

The calculations can be continued now by expanding the equation inside the integral in a power series of r . In this research the expansion was performed up to the second order around a point q , the middle point of the trajectory. The result, after integrating in r , is shown below in the complete form (functions of r_{\min} , r_{\max} , q , μ , and α) because it can be used to compute values for any desirable values of those variables. Because the goal is to obtain only an estimate of the results and because the maximum difference between the first- and second-order expansion is about 7%, only the first-order complete equation is shown here because it has a simpler form:

$$F_1(\alpha) = \left\{ \frac{(1 - \mu)(q + \cos \alpha)}{(2\mu/q)^{\frac{1}{2}}(1 + q^2 + 2q \cos \alpha)^{\frac{3}{2}}} r + (1 - \mu) \left[-\frac{3(q + \cos \alpha)^2}{(2\mu/q)^{\frac{1}{2}}(1 + q^2 + 2q \cos \alpha)^{\frac{5}{2}}} + \frac{\mu(3q + \cos \alpha)}{q^2(2\mu/q)^{\frac{3}{2}}(1 + q^2 + 2q \cos \alpha)^{\frac{3}{2}}} \right] \left(\frac{r^2}{2} - qr \right) \right\}_{r_{\min}}^{r_{\max}} \quad (25)$$

Using the values $r_{\min} = 1,838/384,400$ (100 km above the lunar surface), $r_{\max} = 100,000/384,400$ (100,000 km above the lunar surface, the usual value for the sphere of capture of the moon in the ballistic gravitational capture studies), $\mu = 0.0121$ (Earth-moon system) and $q = (r_{\min} + r_{\max})/2$ (the medium point of the trajectory) the first-order equation obtained is

$$F_1^1(\alpha) = [0.0782 + 0.5902 \cos(\alpha)][1.0176 + 0.2649 \cos(\alpha)]^{-1.5} \quad (26)$$

The equivalent equation for the second-order expansion is shown next because in this form it is not too large:

$$\begin{aligned} F_1(\alpha) = & 0.2836[0.0170 - 0.0730(1.0175 + 0.2649 \cos \alpha) \\ & + 0.3076(1.0175 + 0.2649 \cos \alpha)^2 + 0.0680 \cos \alpha \\ & - 0.0847(1.0175 + 0.2649 \cos \alpha) \cos \alpha + 2(1.0175 \\ & + 0.2649 \cos \alpha)^2 \cos \alpha + 0.0168 \cos 2\alpha - 0.0640(1.0175 \\ & + 0.2649 \cos \alpha) \cos 2\alpha + 0.0212 \cos 3\alpha] \\ & \times (1.0175 + 0.2649 \cos \alpha)^{-\frac{7}{2}} \end{aligned} \quad (27)$$

This equation is plotted as a function of α in Fig. 9. The curve shows a sinusoidal variation of the integral with the most favorable angle for the ballistic gravitational capture close to 180 deg, where the force has the most negative value. It means that the component of this force applied opposite to the motion of the spacecraft has its maximum effect in reducing the final velocity of the spacecraft, then obtaining a capture with the most negative value for the energy.

For the radial component of the centrifugal force, $-(1 - \mu) \cos \alpha + r$, the integral is

$$\begin{aligned} \int_{r_{\min}}^{r_{\max}} \left(\frac{F_{ce}}{V} \right) ds = \int_{r_{\min}}^{r_{\max}} [(\mu - 1) \cos \alpha + r] \left(\frac{2\mu}{r} \right)^{-\frac{1}{2}} dr \\ = \left\{ \left[-0.4r^2 + \frac{2}{3}r(\mu - 1) \cos \alpha \right] \left(\frac{2\mu}{r} \right)^{-\frac{1}{2}} \right\}_{r_{\min}}^{r_{\max}} \end{aligned} \quad (28)$$

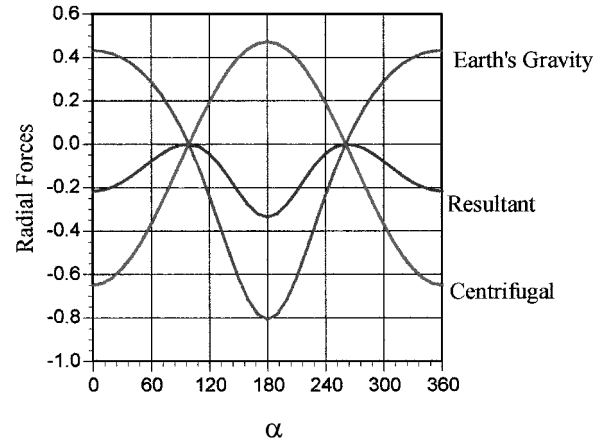


Fig. 9 Integral of the disturbing radial forces (canonical units) vs α (deg).

Using the same values used in the preceding situation for the variables, this last equation can be reduced to

$$F_2(\alpha) = -0.0887 - 0.5603 \cos \alpha \quad (29)$$

This equation is plotted as a function of α in Fig. 9. It also shows a sinusoidal variation of the integral, with the most favorable angle for the ballistic gravitational capture at zero and 360 deg (the most negative values of the integral). It means that at those points the component of the centrifugal force acting opposite to the motion of the spacecraft has its maximum effect. The sign of the values is always opposite to the sign of the effect of the gravity of the Earth, which means that the effects are working against each other. Adding the radial effects of both forces, the equation for the resultant force in the radial direction is obtained. This force will be called $F_3(\alpha)$, and it is also plotted as a function of α in Fig. 9. From those results it is clear that the integral of the total effect is always negative, which means that the spacecraft always has its velocity reduced by the perturbation. It is never increased. There are two points where the integral of the effect is null, which means that the two perturbing forces acting on the spacecraft cancel each other and it travels as if there were no perturbations at all. In this figure it is also possible to obtain the best point to perform the ballistic gravitational capture. This point is at $\alpha = 180$ deg, which has the strongest accumulated effect for the resultant force.

After that some calculations are developed to obtain the equivalent equations for the transverse direction, in the same way that was done with the radial components. In this case the difference between first- and second-order expansions has a maximum of 4%. The analytical equation for the first-order expansion is

$$\begin{aligned} F_4(\alpha) = \int_{r_{\min}}^{r_{\max}} \frac{(1 - \mu) \sin \alpha}{(2\mu/r)^{\frac{1}{2}}(1 + r^2 + 2r \cos \alpha)^{\frac{3}{2}}} dr \\ = \left\{ \frac{(1 - \mu) \sin \alpha}{(2\mu/q)^{\frac{1}{2}}(1 + q^2 + 2q \cos \alpha)^{\frac{3}{2}}} r + (1 - \mu) \right. \\ \times \left[-\frac{(q + \cos \alpha)}{(1 + q^2 + 2q \cos \alpha)^{\frac{3}{2}}} + \frac{1}{2q(1 + q^2 + 2q \cos \alpha)^{\frac{1}{2}}} \right] \\ \times \left(\frac{2\mu}{q} \right)^{-\frac{1}{2}} \sin \alpha \left(\frac{r^2}{2} - qr \right) \left. \right\}_{r_{\min}}^{r_{\max}} \end{aligned} \quad (30)$$

Then, using the same numerical values for the variables used for the radial component the equation obtained is

$$F_4^1(\alpha) = 0.5902 \sin(\alpha)[1.0176 + 0.2649 \cos(\alpha)]^{-\frac{1}{2}} \quad (31)$$

For the second-order expansion the equivalent result is

$$F_4(\alpha) = \left\{ \frac{0.0025}{(1.0175 + 0.2649 \cos \alpha)^{\frac{5}{2}}} - \frac{0.0032}{(1.0175 + 0.2649 \cos \alpha)^{\frac{3}{2}}} + \frac{0.5674}{(1.0175 + 0.2649 \cos \alpha)^{\frac{1}{2}}} + \left[\frac{0.0013}{(1.0175 + 0.2649 \cos \alpha)^{\frac{5}{2}}} - \frac{0.0121}{(1.0175 + 0.2649 \cos \alpha)^{\frac{3}{2}}} \right] \cos \alpha + \frac{0.0024 \cos 2\alpha}{(1.0175 + 0.2649 \cos \alpha)^{\frac{5}{2}}} \right\} \sin \alpha \quad (32)$$

For the centrifugal force the integral of the function $(\mu - 1) \sin(\alpha)(2\mu/r)^{-1/2}$ can be evaluated in a closed form to give

$$F_5(\alpha) = \left[\frac{2}{3} r(\mu - 1) \sin \alpha (2\mu/r)^{-\frac{1}{2}} \right]_{r_{\min}}^{r_{\max}} \quad (33)$$

Then, using the numerical values available the equation obtained is

$$F_5(\alpha) = -0.5603 \sin \alpha$$

For the coriolis force ($F_{C_0} = -2\omega \times V$) the result is

$$F_6(\alpha) = \int_{r_{\min}}^{r_{\max}} \left(\frac{F_{C_0}}{V} \right) dr = \int_{r_{\min}}^{r_{\max}} 2 dr = 2r \Big|_{r_{\min}}^{r_{\max}} = 0.5107 \quad (34)$$

Adding the three transverse perturbing forces, the resultant force can be obtained. This force will be called $F_7(\alpha)$. Numerical simulations show that the magnitude of the total effect of the transverse perturbing force is dominated by the coriolis force, which means that it is not negligible and that the assumption of radial trajectories has to be seen as an estimate of the reduction of C_3 for the system considered and is not a good approximation for an individual trajectory.

The next step to be developed here is to obtain an analytical equation to predict the variation of C_3 as a function of the angle α , using Eq. (20). To do that, it is necessary to obtain the value of the integral effect of the gravitational force of the moon in the direction of motion of the spacecraft under the assumption of radial motion. The gravitational force of the moon acts only in the radial direction with a magnitude given by $F_M = \mu/r^2$. So, its integral effect with respect to time is given by (using the same numerical value used before for μ , r_{\max} , and r_{\min})

$$\int_{t_0}^{t_f} F dt = \int_{r_{\min}}^{r_{\max}} \left(\frac{F}{V} \right) dr = \sqrt{\frac{\mu}{2}} \int_{r_{\min}}^{r_{\max}} r^{-\frac{3}{2}} dr = 1.94471 \quad (35)$$

Then, the total effect I_{tot} is given by $F_3(\alpha) + 1.94471$, where $F_3(\alpha)$ is given by $F_1(\alpha) + F_2(\alpha)$ [Eqs. (26) and (27)]. Equation (20) becomes (using the numerical values available) $-4.968172 + 4.499421I_{\text{tot}} - I_{\text{tot}}^2$, which completes the required derivation.

Estimating the Reduction of C_3 for Different Systems of Primaries

The analytical equations just obtained can be used to estimate the reduction of C_3 as a function of the mass parameter μ , which identifies the system of primaries used as the mathematical model. To perform this estimate, the distance of the sphere of capture r_{\max} and the periapsis distance r_{\min} of the trajectory are given¹¹ by $(2\mu)^{1/3}$ and $(2\mu)^{1/3}/20$, respectively. Consider also that there is an ideal trajectory that is radial and traveling with $\alpha = 180$ deg, that is the radial direction that provides the maximum decrease of C_3 , as shown

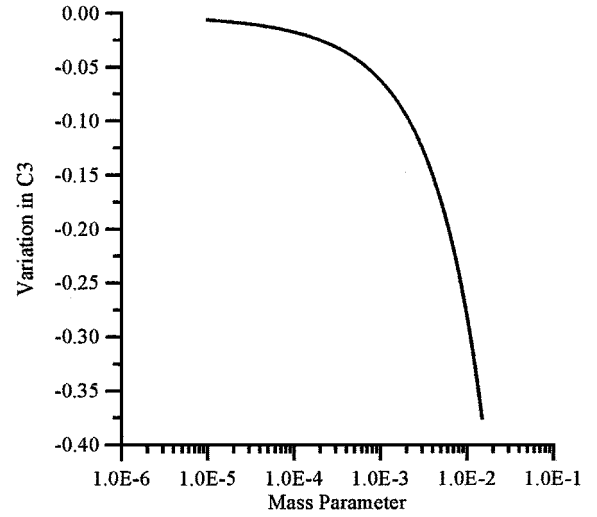


Fig. 10 Analytical estimate for the variation of C_3 as a function of the mass parameter.

before in this paper. Then, the resultant radial force given by Eq. (25) added to Eq. (28) becomes

$$F(\mu) = k^{-\frac{3}{2}} \left[-44054 + k^{\frac{3}{2}} (0.6592 - 0.5037\mu^{\frac{1}{3}} - 0.6592\mu) + 29140\mu^{\frac{1}{3}} + 44054\mu - 29140\mu^{\frac{4}{3}} \right] \quad (36)$$

where $k = 1600 - 2117\mu^{1/3} + 700\mu^{2/3}$. The equation for the variation of C_3 in the rotating frame is given by Eq. (29), using $V_p = \sqrt{(2\mu/r_p)}$ and

$$I_{\text{tot}} = F(\mu) + \sqrt{\frac{\mu}{2}} \int_{(2\mu)^{\frac{1}{3}}/20}^{(2\mu)^{\frac{1}{3}}} r^{-\frac{3}{2}} dr = F(\mu) + 4.3746\mu^{\frac{1}{3}}$$

Then, this variation is converted to the inertial frame using Eq. (21) at the periapsis (where $x = -r_{\min} + \mu$, $\dot{x} = \sqrt{(2\mu/r_{\min})}$, $y = \dot{y} = 0$) and at the sphere of capture (where $x = -r_{\max} + \mu$, $\dot{x} = \sqrt{(2\mu/r_{\max})}$, $y = \dot{y} = 0$). The final result is

$$\Delta C_{3\text{inertial}} = -F^2(\mu) + 2.52F(\mu)\mu^{\frac{1}{3}} + 1.58\mu^{\frac{2}{3}} \quad (37)$$

Figure 10 plots this equation. This analysis confirms the numerical results and the main conclusions stated in the literature (p. 78 of Ref. 11): 1) the reduction of C_3 increases strongly with the mass parameter because the relative effect of the two primaries increases; 2) for values of the mass parameter below 0.0001, the ballistic gravitational capture does not exist for practical purposes. Two more comments related to Fig. 10 are important. First, the value predicted for the Earth-moon system is -0.3217 , and the numerical value (according to Ref. 11, p. 50) is -0.2205 ($-0.22559 \text{ km}^2/\text{s}^2$). The main reason for this difference is that the values used for the periapsis distance and the sphere of capture are different. Using for the analytical and numerical estimates the same values ($r_{\min} = 1,838/384,400$ and $r_{\max} = 100,000/384,400$), the first-order estimate gives a value of -0.2208 , which is a very good result. Second, the values predicted for the sun-Jupiter and sun-Saturn systems are -0.055 and -0.024 , respectively, and the corresponding results from numerical simulations¹¹ are about -0.042 and -0.026 , which is in reasonable agreement for an estimate.

Conclusions

This paper had two main goals when studying the ballistic gravitational capture problem: 1) it showed an explanation of the phenomenon based in the calculation of the forces involved in the dynamics as a function of time and in their integration with respect to time; 2) it derives analytical equations to study this problem under the assumption of radial motion, which leads to the derivation of an equation that estimates the reduction of C_3 as a function of the mass parameter of the system of primaries. To achieve the second goal,

the forces acting on the ballistic gravitational capture problem are obtained in closed forms. There are two forces that act as disturbing forces in the direction of motion: the gravitational force caused by the Earth and the centrifugal force. These forces can decelerate the spacecraft, working opposite to its motion. This is equivalent to applying a continuous propulsion force against the motion of the spacecraft. In the radial direction the gravitational force caused by the Earth and the centrifugal force work in opposite directions, but the resultant force always works against the motion of the spacecraft, with the exception of two points where they cancel each other.

Acknowledgments

The author is grateful to Hiroshi Yamakawa for providing a copy of his Ph.D. Dissertation (Ref. 11), which was a valuable source to compare some of the results presented here. Thanks also go to the National Council for Scientific and Technological Development, Brazil, for the Contract 300221/95-9 and to Foundation to Support Research in São Paulo State, Brazil, for the Contract 2000/14769-4.

References

- ¹Belbruno, E. A., "Lunar Capture Orbits, a Method of Constructing Earth Moon Trajectories and the Lunar Gas Mission," AIAA Paper 87-1054, May 1987.
- ²Belbruno, E. A., "Examples of the Nonlinear Dynamics of Ballistic Capture and Escape in the Earth-Moon System," AIAA Paper 90-2896, Aug. 1990.
- ³Belbruno, E. A., "Ballistic Lunar Capture Transfer Using the Fuzzy Boundary and Solar Perturbations: a Survey," *Journal of the British Interplanetary Society*, Vol. 47, 1994, pp. 73-80.
- ⁴Krish, V., "An Investigation into Critical Aspects of a New Form of Low Energy Lunar Transfer, the Belbruno-Miller Trajectories," M.S. Thesis, Dept. of Mechanical Engineering, Massachusetts Inst. of Technology, Cambridge, MA, Dec. 1991.
- ⁵Krish, V., Belbruno, E. A., and Hollister, W. M., "An Investigation into Critical Aspects of a New Form of Low Energy Lunar Transfer, the Belbruno-Miller Trajectories," *Proceedings of the AIAA/AAS Astrodynamics Conference*, AIAA, Washington, DC, 1992, pp. 435-444.
- ⁶Miller, J. K., and Belbruno, E. A., "A Method for the Construction of a Lunar Transfer Trajectory Using Ballistic Capture," *American Astronautical Society*, Paper 91-100, Feb. 1991.
- ⁷Belbruno, E. A., and Miller, J. K., "A Ballistic Lunar Capture for the Lunar Observer," Jet Propulsion Lab., JPL IOM 312/90.4-1752, Internal Document, Pasadena, CA, Aug. 1990.
- ⁸Belbruno, E. A., and Miller, J. K., "Sun-Perturbed Earth-to-Moon Transfers with Ballistic Capture," *Journal of Guidance, Control, and Dynamics*, Vol. 16, No. 4, 1993, pp. 770-775.
- ⁹Yamakawa, H., Kawaguchi, J., Ishii, N., and Matsuo, H., "A Numerical Study of Gravitational Capture Orbit in Earth-Moon System," *American Astronautical Society*, Paper 92-186, Feb. 1992.
- ¹⁰Yamakawa, H., Kawaguchi, J., Ishii, N., and Matsuo, H., "On Earth-Moon Transfer Trajectory with Gravitational Capture," *American Astronautical Society*, Paper 93-633, Aug. 1993.
- ¹¹Yamakawa, H., "On Earth-Moon Transfer Trajectory with Gravitational Capture," Ph.D. Dissertation, Dept. of Aeronautics, Univ. of Tokyo, Japan, Dec. 1992.
- ¹²Kawaguchi, J., "On the Weak Stability Boundary Utilization and Its Characteristics," *American Astronautical Society*, Paper 00-176, Jan. 2000.
- ¹³Belbruno, E. A., and Miller, J. K., "A Ballistic Lunar Capture Trajectory for Japanese Spacecraft Hiten," Jet Propulsion Lab., JPL IOM 312/90.4-1731, Internal Document, Pasadena, CA, June 1990.
- ¹⁴Vieira Neto, E., and Prado, A. F. B. A., "A Study of the Gravitational Capture in the Restricted-Problem," *Proceedings of the International Symposium on Space Dynamics*, edited by J.-P. Carrou, Cépaduès-Éditions, Toulouse, France, 1995, pp. 613-622.
- ¹⁵Vieira Neto, E., and Prado, A. F. B. A., "Time-of-Flight Analyses for the Gravitational Capture Maneuver," *Journal of Guidance, Control, and Dynamics*, Vol. 21, No. 1, 1998, pp. 122-126.
- ¹⁶Vieira Neto, E., "Estudo Numérico da Captura Gravitacional Temporária Utilizando o Problema Restrito de Três Corpos," Ph.D. Dissertation, Dept. of Engineering and Space Technology, Inst. Nacional de Pesquisas Espaciais, Brazil, Aug. 1999.
- ¹⁷Vieira Neto, E., and Prado, A. F. B. A., "Study of the Gravitational Capture in the Elliptical Restricted Three-Body Problem," *Proceedings of the International Symposium on Space Dynamics*, Inst. of Space and Astronautical Science, Japan, 1996, pp. 202-207.
- ¹⁸Belbruno, E. A., "The Dynamical Mechanism of Ballistic Lunar Capture Transfers in the Four-Body Problem from the Perspective of Invariant Manifolds and Hill's Regions," *Inst. D'Estudis Catalans, CRM Research Rept. 270*, Barcelona, Nov. 1994.
- ¹⁹Sweetser, T. H., Maddock, R., Johannesen, J., Bell, J., Penzo, P. A., Wolf, A., Williams, S. N., Matousek, S., and Weinstein, S., "Trajectory Design for a Europa Orbiter Mission: A Plethora of Astrodynamics Challenges," *Advances in Astronautical Science, Spaceflight Mechanics*, Vol. 95, edited by K. C. Howell, D. A. Cicci, J. E. Cochran Jr., and T. S. Kelso, Univelt, San Diego, CA, 1997, pp. 901-919.
- ²⁰Koon, W. S., Lo, M. W., Marsden, J. E., and Ross, S. D., "Heteroclinic Connections Between Periodic Orbits and Resonance Transitions in Celestial Mechanics," *Chaos*, Vol. 10, 2000, pp. 427-469.
- ²¹Belbruno, E. A., "Low Energy Trajectories for Space Travel and Stability Transition Regions," *IFAC Workshop on Lagrangian and Hamiltonian Methods for Nonlinear Control*, Elsevier Science, Oxford, England, U.K., March 2000.
- ²²Belbruno, E. A., "Analytic Estimation and Geometry of Weak Stability Boundaries with Several Mission Applications," Jet Propulsion Lab., Contract 1213585: JPL Interim Rept. 2, Pasadena, CA, June 2000.
- ²³Bello-Mora, M., Graziani, F., Teofilatto, P., Circi, C., Porfilio, M., and Hechler, M., "A Systematic Analysis on Weak Stability Boundary Transfers to the Moon," *Proceedings of 51st International Astronautical Congress*, 2000.
- ²⁴Mendell, W., "The Weak Stability Boundary, a Gateway for Human Exploration of Space," *Proceedings of 51st International Astronautical Congress*, 2000.
- ²⁵Belbruno, E. A., Humble, R., and Coil, J., "Ballistic Capture Lunar Transfer Determination for the U.S. Air Force Academy Blue Moon Mission," *Advances in Astronautical Science, Spaceflight Mechanics*, Vol. 95, edited by K. C. Howell, D. A. Cicci, J. E. Cochran Jr., and T. S. Kelso, Univelt, San Diego, CA, 1997, pp. 869-880.
- ²⁶Szebehely, V. G., *Theory of Orbits*, Academic Press, New York, 1967, pp. 7-41.
- ²⁷Prado, A. F. B. A., "Optimal Transfer and Swing-By Orbits in the Two- and Three-Body Problems," Ph.D. Dissertation, Dept. of Aerospace Engineering and Engineering Mechanics, Univ. of Texas at Austin, TX, Dec. 1993.